Applied Physics Letters ARTICLE pubs.aip.org/aip/apl

Full counting statistics of ultrafast quantum transport

Cite as: Appl. Phys. Lett. **123**, 034006 (2023); doi: 10.1063/5.0152161
Submitted: 28 March 2023 · Accepted: 25 June 2023 ·
Published Online: 19 July 2023

M. Hübler and W. Belzig[a)]

AFFILIATIONS

Fachbereich Physik, Universitat Konstanz, D-78457 Konstanz, Germany

Note: This paper is part of the APL Special Collection on Electronic Noise: From Advanced Materials to Quantum Technologies.
[a)]**Author to whom correspondence should be addressed:** Wolfgang.Belzig@uni-konstanz.de

ABSTRACT

Quantum transport in the presence of time dependent drives is dominated by quantum interference and many body effects at low tempera tures. For a periodic driving, the analysis of the full counting statistics revealed the elementary events that determine the statistical properties of the charge transport. As a result, the noise correlations display quantum oscillation as functions of the ratio of the voltage amplitude and the drive frequency, reflecting the detailed shape of the drive. However, so far only continuous wave excitations were considered, but, recently, transport by few cycle light pulses were investigated, and the need for a statistical interpretation became eminent. We address the charge transfer generated by single or few cycle light pulses. The fingerprints of these time dependent voltage pulses are imprinted in the full counting statistics of a coherent mesoscopic conductor at zero temperature. In addition, we identify the elementary processes that occur in the form of electron hole pair creations, which can be investigated by the excess noise. We study the quantum oscillations in the differen tial noise induced by a wave packet consisting of an oscillating carrier modulated by a Gaussian or a box shaped envelope. As expected, the differential noise exhibits an oscillatory behavior with increasing amplitude. In particular, we find clear signature of the so called carrier envelope phase in the peak heights and positions of these quantum oscillations. More carrier cycles under the Gaussian envelope diminish the influence of the carrier envelope phase, while this is not true for the box pulses, probably related to the abrupt onset.

Oscillating electric fields impact the electron transport in meso scopic conductors, which leads to features at multiples of the driving fre quency.[1–3] A mesoscopic conductor divides the incident electron stream from the terminals according to its total transmission probabilities.[4] These charge carriers are distributed by the equilibrium Fermi function, i.e., by the chemical potentials and temperatures of their departure ter minals. Photon assisted transport describes electron tunneling driven by an oscillating chemical potential.[5,6] The electron wave function at energy E exhibits side bands at energies $E + nh\omega, n \in \mathbb{Z}$, weighted by Bessel functions.[4–6] This leads to kinks at voltages $nh\omega/e$ in the zero temperature noise. The step height in the differential noise depends on the ac amplitude through the Bessel functions,[2,4] which can be general ized beyond the simple scattering picture.[7–9] These observations are complemented by the dynamical response of the shot noise[10,11] or per turbative generalizations to interacting conductors.[12–14]

Going beyond the noise and analyzing the full counting statistics (FCS) gives insight into the elementary processes involved in electron transport.[15–18] Similar to the photon counting statistics, FCS represents the electron counting statistics and is the probability distribution of tra versed charge. The difference between the transfer of classical charge carriers or quantum mechanical particles obeying the Fermi statistics manifests itself in the FCS, where the former obey a Poisson distribu tion, while the latter follow a binomial distribution.[15,16,19] In the limit of small transmission, the binomial distribution approaches a Poisson dis tribution, and the quantum properties get lost. The difference is seen in the suppression of the shot noise, as indicated by the Fano factor. In superconducting junctions, the FCS can assume negative values, which is inconsistent with the notion of a probability distribution.[17] Nevertheless, this function accounts for all elementary processes and can in principle be measured in an experiment. The information about the charge transport is contained in the cumulant generating function (CGF). Dismantling the CGF into a sum of binomials or multinomials unveils the independent elementary processes at play. This shows, for instance, that the charge transfer in spin sensitive tunnel junctions is carried by single electrons and spin singlet pairs when the electron source is a mesoscopic conductor in series.[18,20]

Time dependent voltage pulses generate collective excitations of the Fermi sea, which are realized as a superposition of electron and hole excitations.[16,19,21] For example, levitons are soliton like electron excitations created by Lorentzian voltage pulses with a quantized flux.[16,19] These states minimize the noise, which is reduced to a corre sponding dc noise. Furthermore, the entire full counting statistic shortens to a corresponding dc statistic.[22,23] Levitons have been real ized experimentally[24] and analyzed via quantum state tomography.[25] In general, many body electronic states generated by a time dependent voltage are built from single electron and electron hole quasiparticle excitations.[21,26] The amplitudes and probabilities of these elementary excitations depend on the details of the drive and can be examined experimentally.[21] The entanglement can be addressed by a continuous variable entanglement test.[27]

Arbitrary time dependent voltages can be treated by the non equilibrium Green's function method.[17,22,23,28] The work[22,23] investi gated the FCS for cosine, square, triangle, sawtooth, and Lorentzian pulses. Apart from a dc statistic, there appears to be a bidirectional part that depends on the scattering of electron hole pairs. The proba bilities of creating these electron hole pairs enter the CGF and are determined by the shape of the pulses. A similar CGF structure is found for a superconductor (S) normal metal (N) contact, because the problem can be mapped onto a NN contact by replacing the transmis sion probabilities with the Andreev reflection probabilities and dou bling the counting field as well as the applied voltage.[29]

Nowadays, light fields can be manipulated on femtosecond time scales, leading to ultrafast electron transport in mesoscopic constrictions. The experiments[30–32] harnessed the nonlinear I V characteristic of their bow tie antenna to establish carrier envelope phase (CEP) control of electron transfer. For a cosine shaped carrier to envelope configuration (CEP $= 0$), the average current is maximal, while for a sine shaped con figuration (CEP $= \pi/2$), the average current vanishes. The near field in the gap is distorted compared to the far field, leading to a strong field enhancement and a shift in the effective carrier envelope phase.[31] A small dc bias can be exploited to direct the photocurrent.[32]

Our work is strongly motivated by the achievements[30–32] and extends the investigations[22,23] to include pulses that are only a few cycles long and modulated by a Gauss or box shaped envelope. With only a few carrier cycles, the phase shift between carrier and envelope (CEP) is expected to have a measurable influence. We are interested in the carrier envelope phase control of electron transfer through a meso scopic conductor. In contrast to studies in Refs. 30 32, this work deals with a linear I V characteristic such that the average current vanishes and the noise is the first nonzero cumulant. The whole full counting statistic is determined by the electron hole pair creation probabilities. We calculate these probabilities for a Gaussian and box pulse and focus on the influence of the carrier envelope phase on the zero temperature noise. As expected, the differential noise shows oscillations with increasing ac amplitude. For both envelopes, the carrier envelope phase clearly affects these oscillations. The influence of the carrier envelope phase attenuates for rising number of carrier cycles under the Gauss. This trend is not seen for the box pulse, proba bly because the temporal behavior at the edges of the box is fundamen tally different for a sine and cosine carrier.

The article is structured as follows: First, we recapitulate the methods[22,23] dealing with the FCS in the context of time dependent voltages. Then we consider the electron hole pair creation probabilities and the differential noise for Gauss and box pulses with a single or few cycles of the carrier frequency, with particular emphasis on the effect of the CEP. Finally, we summarize our findings and give an outlook.

The full counting statistic is concerned with the probability of charge transfer.[15,16] The transfer of N charges in a given measurement time t_0 is described by the probability density $P_{t_0}(N)$. For uncorrelated and unidirectional transport, we get a Poissonian distribution that exhibits Schottky's shot noise. In contrast, for a degenerated electron gas at zero temperature, we obtain a binomial distribution.

All information about the cumulants is encoded in the cumulant generating function (CGF) $\mathscr{S}(\chi)$, which is related to the probability density by

$$\exp(\quad \mathscr{S}(\chi)) = \sum_N P_{t_0}(N)\exp(iN\chi) \tag{1}$$

with the counting field χ, and the imaginary unit i.[15,16] The normaliza tion of the distribution requires $\mathscr{S}(0) = 0$. The cumulants are attained by

$$C_n = \quad (\quad i)^n \frac{\partial^n}{\partial \chi^n} \mathscr{S}(\chi)|_{\chi\ 0}, \tag{2}$$

where the first cumulant $C_1 = N := \sum_N NP_{t_0}(N)$ is the mean value, the second cumulant $C_2 = \overline{(N \quad N)^2}$ is the noise. Expressed by the current operator $\hat{I}(t)$ at time t, the first cumulant corresponds to

$$C_1 = \frac{1}{e}\int_0^{t_0} dt\langle \hat{I}(t)\rangle, \tag{3}$$

and the second cumulant corresponds to

$$C_2 = \frac{1}{2e^2}\int_0^{t_0}\int_0^{t_0} dtdt'\langle\{\Delta\hat{I}(t), \Delta\hat{I}(t')\}\rangle, \tag{4}$$

with $\Delta\hat{I}(t) = \hat{I}(t) \quad \langle\hat{I}(t)\rangle$, $\{\cdot,\cdot\}$ being the anticommutator, and e, the elementary charge.

In a coherent mesoscopic conductor, the CGF depends on an ensemble of transmission eigenvalues $\{T_n\}$ and on the quasiclassical Green's functions of the terminals.[17,28] The Green's function is deter mined by the Fermi distribution, i.e., by the chemical potential and the temperature of the corresponding terminal. If we apply a dc bias between the terminals, then each energy contributes separately to the CGF, where the bias enters the Fermi distribution as the difference between the chemical potentials.

Time dependent voltages $V(t)$ correlate transport at different energies, and the CGF depends on their entire shape.[22,23,29] We include time dependent voltages via a gauge like transformation of one Green's function, similar to the counting field. The transformed Fermi function has no longer a diagonal structure in energy represen tation. The CGF does not decouple between different energies and remains a complex convolution sum. In the zero temperature limit, this can be solved for periodic voltages by a diagonalization procedure, described in detail in Refs. 22 and 23. Within the measurement time t_0, we consider a large train of well separated voltage pulses with a repetition period $\tau = 2\pi/\Omega$. The CGF $\mathscr{S}(\chi)/(t_0\Omega/\pi) = \mathscr{S}_{\mathrm{uni}}(\chi) + \mathscr{S}_{\mathrm{bi1}}(\chi) + \mathscr{S}_{\mathrm{bi2}}(\chi)$ per pulse and spin subdivide into a unidirec tional part,

$$\mathscr{S}_{\mathrm{uni}}(\chi) = N_{\mathrm{uni}} \sum_n \ln\left[1 + T_n(e^{-ik\chi} \quad 1)\right] \tag{5}$$

and bidirectional parts,

$$\mathscr{S}_{\mathrm{bi1,2}}(\chi) = N_{\mathrm{bi1,2}} \sum_n \sum_k \ln\left[1 \quad T_n R_n p_{k1,2}(e^{i\chi} \quad 1)(e^{-i\chi} \quad 1)\right]. \tag{6}$$

The numbers of attempts per pulse and spin are given by $N_{\mathrm{uni}} = |eV|/\Omega$, $N_{\mathrm{bi1}} = \Omega_1/\Omega$ and $N_{\mathrm{bi2}} = (1 \quad \Omega_1/\Omega)$, where $\Omega_1 = eV \quad \lfloor eV/\Omega \rfloor \Omega$, with $\lfloor x \rfloor$ being the floor of the real number x. In the formulas, the average voltage $V = (1/\tau)\int_{-\tau/2}^{\tau/2} V(t)dt$, the probabilities $p_{k1,2}$ of creating an electron hole pair, and the reflection probabilities $R_n = 1 \quad T_n$ occur. The parameter $\kappa = 1$ ($\kappa = \quad 1$) indicates the direction of charge transfer, determined by $eV > 0$ ($eV < 0$). We set $\mathrm{h} = 1$ in all expressions. The bidirectional FCS (6) is completely determined by the electron hole pair creation probabilities, which carry the details of the drive shape. In contrast, the unidirectional FCS is only determined by the average voltage V.

Unidirectional transport (5) corresponds to a single electron transfer with probability T_n, where each transport channel contributes independently. Within the measurement time t_0, there are $t_0|eV|/\pi$ attempts of electrons to cross the conductor. Hence, unidirectional charge transfer only occurs at finite average voltages V. The period τ and the characteristic correlation time of the current fluctuations are assumed to be much smaller than the measurement time. For a single transport channel, the CGF translates to a binomial distribution.

Bidirectional charge transport (6) stems from two particle processes, namely, the creation of electron hole pairs in one terminal by the ac voltage $\Delta V(t) = V(t) \quad V$. This pair contributes to the statistics if the electron traverses the conductor and the hole gets reflected, or vice versa. This process is captured by the probability $T_n R_n p_k$, which is composed of the transmission probability T_n, the reflection probability R_n, and the probability p_k of creating an electron hole pair. The index k labels different electron hole pair excitations of the Fermi sea.[21] We have to encounter two types of bidirectional processes. They differ by the number of attempts $N_{\mathrm{bi1,2}}$ and electron hole pair creation probability $p_{k1,2}$. In contrast to the unidirectional charge transport, the bidirectional parts only contribute to the noise and higher order even cumulants.

The details of the time dependent drive determine the probabilities of electron hole pair creation. We obtain the probabilities p_k by diagonalizing the matrix,

$$M_{nm}(E) = \mathrm{sgn}(E + n\Omega) \sum_{k \quad \infty}^{\infty} a_{n+k} a^*_{m+k} \mathrm{sgn}(E \quad k\Omega \quad eV), \tag{7}$$

with the signum function $\mathrm{sgn}(\cdot)$, a_n^* being the complex conjugate of a_n and the coefficients,

$$a_n = \frac{(\quad 1)^n}{\tau} \int_{-\tau/2}^{\tau/2} dt \exp\left[\quad i \int_{-\tau/2}^{t} dt' e\Delta V(t')\right] e^{in\Omega t}. \tag{8}$$

The coefficients depend on the ac drive $\Delta V(t) = V(t) \quad V$ and obey the properties

$$\sum_{k \quad \infty}^{\infty} a_{n+k} a^*_{m+k} = \delta_{nm}, \quad \sum_{k \quad \infty}^{\infty} k|a_k|^2 = 0. \tag{9}$$

In the relevant energy range $0 < E < \Omega$, the matrix is piecewise constant for energies $E \in (0, \Omega_1)$, $\Omega_1 = eV \quad \lfloor eV/\Omega \rfloor \Omega$ and $E \in (\Omega_1, \Omega)$. This leads to the two types of bidirectional processes denoted by an index of 1 for the first interval and an index of 2 for the second interval. The matrix M_{nm} is unitary, and, therefore, the eigenvalues assume the form $\exp(\pm i\alpha_{k1,2})$. If the unidirectional number eV/Ω of attempts per cycle and per spin is an integer, then there is only one bidirectional CGF $\mathscr{S}_{\mathrm{bi2}}(\chi)$. The phase $\alpha_{k1,2}$ of the eigenvalues enters directly into the electron hole pair creation probability by $p_{k1,2} = \sin^2(\alpha_{k1,2}/2)$. The corresponding eigenvectors are related to the electron hole quasiparticle amplitude and dictate the drive induced many body wave function.[21]

The bidirectional current current noise is proportional to the sum of all probabilities p_k, which rise to one as the amplitude of the ac drive is increased. In the following, we are concerned with time dependent voltages, which exhibit a vanishing average voltage $V = 0$. Hence, the unidirectional part vanishes, so that on average no charge is transported, and only type 2 bidirectional processes appear. The current current noise per pulse and per spin has the form

$$S = 2e^2 \left(\sum_n T_n R_n\right) \sum_k p_k. \tag{10}$$

Based on the findings in Refs. 22 and 23, we expect oscillatory behavior in the differential noise $\partial S/(\partial(eV_0))$, which fades out for large ac amplitudes. In the region $V_0 \in \mathscr{C}_k$, where $p_k \neq 0$ and $p_k \neq 1$, the drive excited electron and hole are correlated.[21–23] There, the probabilities p_k exhibit an increase from 0 to 1 with rising ac amplitude. Oscillations come from these ramp ups of the probabilities p_k, where the slope determines the height and the turning point determines the position of the peak in $\partial p_k/\partial(eV_0)$. Higher order even cumulants consist of polynomials in p_k. These polynomials still vary within their correlation region $\mathscr{C}_k$ and give rise to oscillations in the higher order even cumulants. However, the repetition of peaks is different than in the noise. All higher order odd cumulants vanish.

We now discuss specific examples using the previously presented formalism. The voltage pulses consist of an oscillating carrier modulated by an envelope. Their displacement against each other is described by the carrier envelope phase (CEP). We are after the effect of the CEP. The voltage assumes the form

$$V(t) = E(t)V_0 \cos(\omega t + \phi) \quad V_{\mathrm{off}} \tag{11}$$

with the envelope $E(t)$, the ac amplitude V_0, the carrier frequency ω, the carrier envelope phase ϕ, the offset $V_{\mathrm{off}} = (1/\tau)\int_{-\tau/2}^{\tau/2} E(t)V_0 \cos(\omega t + \phi)$, and the repetition rate $1/\tau$. The offset is subtracted to ensure a vanishing average voltage.

For the following results, we calculated the coefficients (8) and diagonalized the matrix (7) to obtain the electron hole pair creation probabilities. The sum of the probabilities gives the noise. Numerically, we utilize a finite dimensional matrix to obtain the eigenvalues. Cutoffs for n and m are chosen on a much larger scale than the one on which $|a_n|$ vanishes.

The first envelope we choose is a Gauss curve of the contour,

$$E(t) = \frac{1}{\sqrt{2\pi}} \exp\left(\quad \frac{t^2}{2\sigma^2}\right), \tag{12}$$

where σ^2 corresponds to the variance. An illustration of the Gaussian pulse is depicted in Fig. 1. The envelope shape is controlled by the ratio

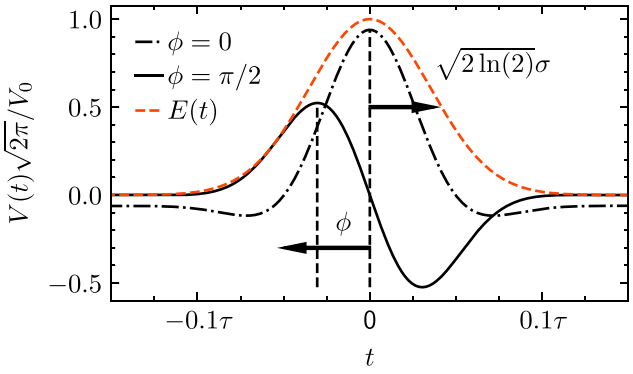

FIG. 1. Gauss pulse and its envelope for carrier envelope phases ϕ 0, $\pi/2$. The ratio between the variance σ and the pulse repetition time τ is chosen as $\tau/(\sqrt{2}\sigma)$ 10. Here, we set $\sigma\omega$ 1, which is a measure of the number of carrier cycles under the Gauss curve. Note the negative offset voltage for ϕ 0 to keep the average voltage at zero.

$\tau/(\sqrt{2}\sigma)$, which determines the relation between the width of the Gauss and the repetition rate. A measure for the number of carrier cycles under the envelope constitutes $\sigma\omega$. The offset voltage is given by

$$V_{\text{off}} = \cos\phi \frac{\sigma}{\tau} V_0 e^{-(\sigma\omega)^2/2} \Re\left[\text{erf}\left(\frac{\tau}{2\sqrt{2}\sigma} \quad \frac{i\sigma\omega}{\sqrt{2}}\right)\right], \qquad (13)$$

with the error function $\text{erf}(\cdot)$, and the real part $\Re[\cdot]$ of a complex number. A maximum is achieved for $\phi = 0$ and a minimum for $\phi = \pi/2$.

The voltage drive $V(t)$ generates electron hole pair excitations of the Fermi sea,[21] which are scattered at the mesoscopic conductor. From the charge statistics, i.e., from the cumulant generating function, we learn the probabilities p_k for creating an electron hole excitation. The upper panel of Fig. 2 illustrates the electron hole creation probabilities p_k and their derivative $\partial p_k/\partial(eV_0)$ for a Gaussian envelope with $\phi = 0$. Within an ac amplitude of $eV_0/\omega \approx 35$, we observe five probabilities, which ramp up successively. Each $k = 1$ to $k = 5$ corresponds to a separate electron hole pair excitation of the Fermi sea. The electron hole pair excitation splits into an uncorrelated electron and hole excitation outside their correlation region $\mathscr{C}_k = \{V_0 | p_k(V_0) \neq 0 \wedge p_k(V_0) \neq 1\}$. The correlation regions and their overlap are better visible in the derivative $\partial p_k/\partial(eV_0)$.

In the following, we focus on the experimentally easier accessible shot noise, which inherits the features of the electron hole pair creation probabilities. The CEP has an observable impact on the differential noise $\partial S/\partial(eV_0)$, depicted in the lower panel of Fig. 2 for carrier envelope phases between $\phi = 0$ and $\phi = \pi/2$. Successive ramp ups of the electron hole pair creation probabilities p_k cause the oscillating character of the differential noise. The CEP has a noticeable influence on the onset of the correlation regions and slope of the ramp ups. This is reflected in the differential noise by the position and height of the peaks, which depend on the details of the drive. For $\phi = 0$, more peaks show up compared to $\phi = \pi/2$, and, therefore, more electron hole pairs are excited for $\phi = 0$. The probabilities p_k for $\phi = 0$ ramp up faster than for $\phi = \pi/2$, which results in higher peaks.

The influence of the CEP diminishes with the increasing number of carrier cycles in a pulse. Figure 3 outlines the dependence of the

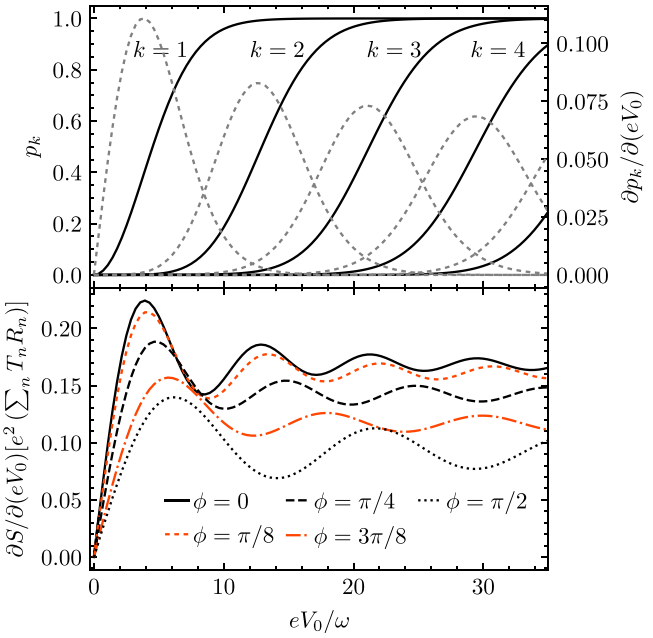

FIG. 2. Upper panel: the electron hole pair creation probabilities p_k (black solid lines) and the corresponding derivatives $\partial p_k/\partial(eV_0)$ (grey dashed lines) as function of the ac amplitude V_0 for a Gaussian envelope function with the carrier envelope phase ϕ 0. Lower panel: the differential noise $\partial S/(\partial(eV_0))$, which is the sum of all $\partial p_k/\partial(eV_0)$. The variance σ in relation to the pulse repetition time τ was set to $\tau/(\sqrt{2}\sigma)$ 10 and in relation to the carrier angular frequency ω to $\sigma\omega$ 1.

differential noise on the number of carrier cycles and their influence on the CEP dependence. For $\sigma\omega = 2$, the curves for $\phi = 0$ and $\phi = \pi/2$ are significantly different, while for rising $\sigma\omega$, they approach each other, and for $\sigma\omega = 7$, they almost overlap. An additional effect is that more probabilities ramp up at the same amplitude eV_0/ω,

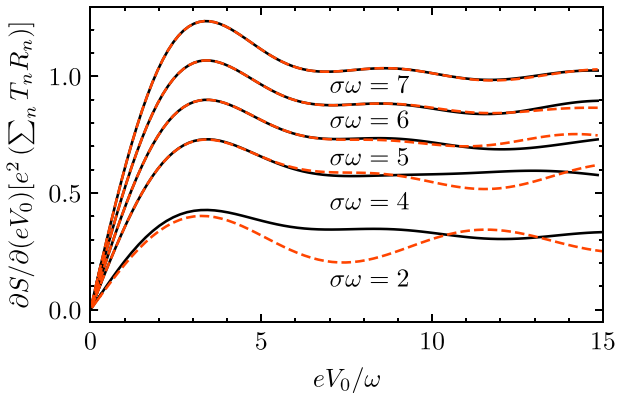

FIG. 3. Differential noise $\partial S/(\partial(eV_0))$ of a Gaussian pulse for different numbers of carrier cycles under the Gaussian envelope. We compare the carrier envelope phase 0 (black solid) to $\pi/2$ (orange dashed) for $\sigma\omega$ 2 to $\sigma\omega$ 7. As the number of carrier cycles increases, the curves with CEP 0 and $\pi/2$ fall on top of each other. Additionally, more elementary processes p_k are contributing, and this leads to an increase in the differential noise. The ratio $\tau/(\sqrt{2}\sigma)$ was fixed at 10.

which shifts the oscillations upward. In comparison to $\sigma\omega = 1$ (see Fig. 2), the second peaks are shifted to lower amplitudes.

The pulses ought to be well separated, i.e., $\tau/(\sqrt{2}\sigma) \gg 1$. In this regime, the differential noise is ideally independent of this parameter. We chose $\tau/(\sqrt{2}\sigma) = 10$ as a trade off between the computational costs and the already independent probabilities in the case of $\phi = \pi/2$. For $\phi = 0$, the probabilities slightly change with increasing $\tau/(\sqrt{2}\sigma) > 10$, presumably due to the non negligible influence of the offset voltage. However, the differences in the oscillations are not exclusively attributable to the offset voltage, because we observe an even smaller period and higher peaks for values $\tau/(\sqrt{2}\sigma) > 10$.

As the second envelope, we study a box of the form

$$E(t) = \Theta(t + N\tau_\omega/2)(1 \quad \Theta(t \quad N\tau_\omega/2)), \tag{14}$$

with $\Theta(\cdot)$ being the Heaviside function, N is the number of carrier cycles in the box, and $\tau_\omega = 2\pi/\omega$ the period of one carrier cycle. The offset voltage vanishes for all carrier envelope phases. Figure 4 depicts the box pulse for CEP $\phi = 0, \pi/2$.

Again, traces of the CEP are pronounced in the differential noise $\partial S/\partial(eV_0)$. The dependence on different carrier envelope phases is shown in the lower panel of Fig. 5. The upper panel of Fig. 5 depicts the electron hole creation probabilities p_k and the derivatives $\partial p_k/\partial(eV_0)$ for $\phi = 0$. The probabilities clearly do not ramp up in an equidistant fashion, and some correlation regions have a larger over lap. These translate in the noise to a nearly hidden second peak for $\phi = 0$ and a merged second peak for $\phi = \pi/8$. The CEP impacts the position and slightly the height of the peaks.

With increasing carrier cycles N in the box, more probabilities p_k ramp up at the same ac amplitude. Therefore, the differential noise experiences an upward shift, akin to the Gaussian envelope. In contrast to the Gaussian pulse, the peak positions remain unchanged for the first few N investigated. The differential noise for $\phi = 0$ and $\phi = \pi/2$ do not approach each other and stay dis tinct. We assume that the origin of this lies in the different behav ior of the cosine and sine at the edges of the box. The cosine ($\phi = 0$) jumps to zero, and the sine ($\phi = \pi/2$) is zero but exhibits a kink.

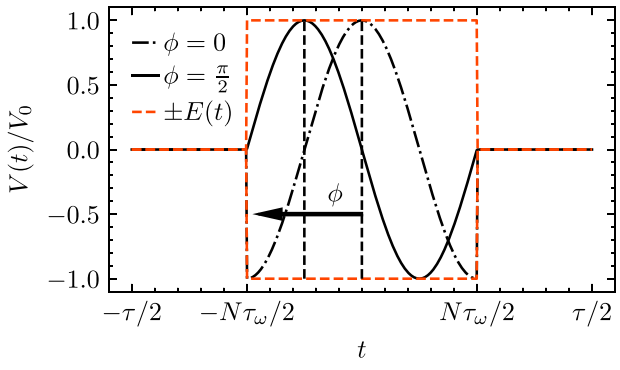

FIG. 4. Illustration of the box pulse and its envelope for carrier envelope phases ϕ 0, $\pi/2$. The box counts N 1 carrier cycles with a period of τ_ω and extends between $N\tau_\omega/2$ and $N\tau_\omega/2$, which is assumed to be smaller than the pulse rep etition time τ.

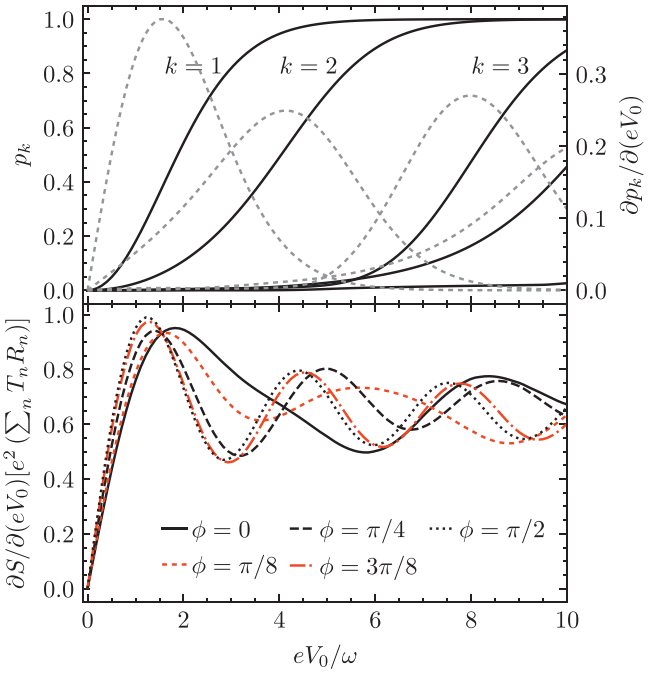

FIG. 5. Upper panel: the electron hole pair creation probabilities p_k (black solid lines) of a box pulse with ϕ 0 and the corresponding derivatives $\partial p_k/\partial(eV_0)$ (gray dashed lines). Lower panel: the differential noise $\partial S/\partial(eV_0)$ for the carrier envelope phases between 0 and $\pi/2$. The differential noise is the sum over all $\partial p_k/\partial(eV_0)$. The number of carrier cycles is N 1. The width of the box in com parison to the pulse repetition rate was fixed to $\tau/(N\tau_\omega)$ 2, because the elec tron hole pair creation probabilities are nearly independent of the box size. Oscillations are caused by the elementary processes that are subsequently acti vated as the voltage amplitude increases.

In conclusion, we have addressed the statistical properties of the current driven by few cycle voltage pulses at the low temperature in a mesoscopic conductor. Explicitly, we have studied single and few cycle pulses with a Gaussian envelope and with a box envelope. The noise is carried by bidirectional processes that lead to an oscillatory behavior of the differential noise. These oscillations strongly depend on the carrier envelope phase, which influences the peak height and position. For the Gaussian pulse, the impact of the CEP decreases with an increasing number of carrier cycles. Noise measurements could be performed in related experiments as in Refs. 30 32 to study the effec tive CEP. As a next goal, it would be intriguing to access the full many body wave function[21] and extract the energy time Wigner function.[33]

We are grateful for discussions with M. Gedamke, S. Großenbach, H. Kempf, A. Leitenstorfer, and A. Moskalenko. This research was supported by the Deutsche Forschungsgemeinschaft (DFG; German Research Foundation) via SFB 1432 (Project No. 425217212).

AUTHOR DECLARATIONS

Conflict of Interest

The authors have no conflicts to disclose.

Author Contributions

Matthias Hübler: Conceptualization (equal); Data curation (equal); Formal analysis (equal); Methodology (equal); Resources (equal); Software (equal); Validation (equal); Visualization (equal); Writing original draft (equal); Writing review & editing (equal). **Wolfgang Belzig:** Conceptualization (equal); Formal analysis (equal); Investigation (equal); Methodology (equal); Project administration (equal); Supervision (equal); Validation (equal); Writing original draft (equal); Writing review & editing (equal).

DATA AVAILABILITY

The data that support the findings of this study are available from the corresponding author upon reasonable request.

REFERENCES

[1]P. Tien and J. Gordon, "Multiphoton process observed in the interaction of microwave fields with the tunneling between superconductor films," Phys. Rev. **129**, 647 (1963).
[2]G. B. Lesovik and L. S. Levitov, "Noise in an ac biased junction: Nonstationary Aharonov Bohm effect," Phys. Rev. Lett. **72**, 538 541 (1994).
[3]R. Schoelkopf, A. Kozhevnikov, D. Prober, and M. Rooks, "Observation of 'photon-assisted' shot noise in a phase-coherent conductor," Phys. Rev. Lett. **80**, 2437 (1998).
[4]Y. Blanter and M. Büttiker, "Shot noise in mesoscopic conductors," Phys. Rep. **336**, 1 166 (2000).
[5]M. Büttiker, H. Thomas, and A. Prêtre, "Current partition in multiprobe conductors in the presence of slowly oscillating external potentials," Z. Phys. B: Condens. Matter **94**, 133 137 (1994).
[6]M. H. Pedersen and M. Büttiker, "Scattering theory of photon-assisted electron transport," Phys. Rev. B **58**, 12993 13006 (1998).
[7]F. Hekking and J. Pekola, "Finite frequency quantum noise in an interacting mesoscopic conductor," Phys. Rev. Lett. **96**, 056603 (2006).
[8]I. Safi and E. V. Sukhorukov, "Determination of tunneling charge via current measurements," EPL **91**, 67008 (2010).
[9]I. Safi, "Time-dependent transport in arbitrary extended driven tunnel junctions," arXiv:1401.5950 (2014).
[10]J. Gabelli and B. Reulet, "Dynamics of quantum noise in a tunnel junction under ac excitation," Phys. Rev. Lett. **100**, 026601 (2008).
[11]J. Hammer and W. Belzig, "Quantum noise in ac-driven resonant-tunneling double-barrier structures: Photon-assisted tunneling versus electron antibunching," Phys. Rev. B **84**, 085419 (2011).
[12]E. V. Sukhorukov, G. Burkard, and D. Loss, "Noise of a quantum dot system in the cotunneling regime," Phys. Rev. B **63**, 125315 (2001).
[13]I. Safi, "Driven quantum circuits and conductors: A unifying perturbative approach," Phys. Rev. B **99**, 045101 (2019).
[14]I. Safi, "Driven strongly correlated quantum circuits and Hall edge states: Unified photoassisted noise and revisited minimal excitations," Phys. Rev. B **106**, 205130 (2022).
[15]L. Levitov and G. Lesovik, "Charge distribution in quantum shot noise," JETP Lett. **58**, 230 235 (1993).
[16]L. S. Levitov, H. Lee, and G. B. Lesovik, "Electron counting statistics and coherent states of electric current," J. Math. Phys. **37**, 4845 4866 (1996).
[17]W. Belzig and Y. V. Nazarov, "Full counting statistics of electron transfer between superconductors," Phys. Rev. Lett. **87**, 197006 (2001).
[18]A. D. Lorenzo and Y. V. Nazarov, "Full counting statistics with spin-sensitive detectors reveals spin singlets," Phys. Rev. Lett. **94**(1), 4 (2005).
[19]D. A. Ivanov, H. W. Lee, and L. S. Levitov, "Coherent states of alternating current," Phys. Rev. B **56**, 6839 6850 (1997).
[20]G. Burkard, D. Loss, and E. V. Sukhorukov, "Noise of entangled electrons: Bunching and antibunching," Phys. Rev. B **61**, R16303 R16306 (2000).
[21]M. Vanević, J. Gabelli, W. Belzig, and B. Reulet, "Electron and electron-hole quasiparticle states in a driven quantum contact," Phys. Rev. B **93**, 041416 (2016).
[22]M. Vanević, Y. V. Nazarov, and W. Belzig, "Elementary events of electron transfer in a voltage-driven quantum point contact," Phys. Rev. Lett. **99**, 076601 (2007).
[23]M. Vanević, Y. V. Nazarov, and W. Belzig, "Elementary charge-transfer processes in mesoscopic conductors," Phys. Rev. B **78**, 245308 (2008).
[24]J. Dubois, T. Jullien, F. Portier, P. Roche, A. Cavanna, Y. Jin, W. Wegscheider, P. Roulleau, and D. Glattli, "Minimal-excitation states for electron quantum optics using levitons," Nature **502**, 659 663 (2013).
[25]T. Jullien, P. Roulleau, B. Roche, A. Cavanna, Y. Jin, and D. Glattli, "Quantum tomography of an electron," Nature **514**, 603 607 (2014).
[26]J. Gabelli and B. Reulet, "Shaping a time-dependent excitation to minimize the shot noise in a tunnel junction," Phys. Rev. B **87**, 075403 (2013).
[27]H. Zhan, M. Vanevic, and W. Belzig, "Continuous-variable entanglement test in driven quantum contacts," Phys. Rev. Lett. **122**, 236801 (2019).
[28]Y. V. Nazarov, "Novel circuit theory of Andreev reflection," Superlattices Microstruct. **25**, 1221 1231 (1999).
[29]W. Belzig and M. Vanevic, "Elementary Andreev processes in a driven superconductor-normal metal contact," Physica E **75**, 22 27 (2016).
[30]T. Rybka, M. Ludwig, M. F. Schmalz, V. Knittel, D. Brida, and A. Leitenstorfer, "Sub-cycle optical phase control of nanotunnelling in the single-electron regime," Nat. Photonics **10**, 667 670 (2016).
[31]M. Ludwig, G. Aguirregabiria, F. Ritzkowsky, T. Rybka, D. C. Marinica, J. Aizpurua, A. G. Borisov, A. Leitenstorfer, and D. Brida, "Sub-femtosecond electron transport in a nanoscale gap," Nat. Phys. **16**, 341 345 (2020).
[32]M. Ludwig, A. K. Kazansky, G. Aguirregabiria, D. C. Marinica, M. Falk, A. Leitenstorfer, D. Brida, J. Aizpurua, and A. G. Borisov, "Active control of ultrafast electron dynamics in plasmonic gaps using an applied bias," Phys. Rev. B **101**, 241412 (2020).
[33]D. Ferraro, A. Feller, A. Ghibaudo, E. Thibierge, E. Bocquillon, G. Fève, C. Grenier, and P. Degiovanni, "Wigner function approach to single electron coherence in quantum Hall edge channels," Phys. Rev. B **88**, 205303 (2013).